Low-cost and miniature all-silica Fabry–Perot pressure sensor for intracranial pressure measurement

Yuting Li (李玉婷)[1], Wentao Zhang (张文涛)[1*], Zhaogang Wang (王兆刚)[1], Hongbin Xu (许红彬)[2], Jing Han (韩晶)[2], and Fang Li (李芳)[1]

[1]*Optoelectronics System Laboratory, Institute of Semiconductors, Chinese Academy of Sciences, Beijing 100083, China*

[2]*Key Laboratory of Structure Health Monitoring and Control of Hebei Province, Shijiazhuang Tiedao University, Shijiazhuang 050043, China*

**Corresponding author: zhangwt@semi.ac.cn*

Received May 2, 2014; accepted July 25, 2014; posted online October 28, 2014

The monitoring of increased intracranial pressure (ICP) is necessary in the diagnosis and treatment of patients with neurological disease because it can provide an insight into the mechanism of the head injury. In this letter, we develop a novel miniature Fabry–Perot (F-P) sensor for ICP measurement. The proposed sensor is fabricated by using a commercially available fusion splicer and a fiber cleaver, by which many difficult art problems involved in fabrication are solved and the online monitoring of the F-P cavity is actualized. The sensor exhibits a linear response to the applied pressure over the range of 0–25 kPa (ample for ICP measurement), with a sensitivity of 10.18 nm/kPa, a resolution of 0.1 kPa, and a reduced thermal sensitivity of 0.068 nm/°C, which shows it can meet the requirements of ICP measurement.

OCIS codes: 060.2370, 280.5475.

DOI: 10.3788/COL201412.111401.

For a supine adult, intracranial pressure (ICP) is normally 0.9–2 kPa. Various neurological disorders can result in the increase of ICP. In the neurosurgical and neurological assessment, the monitoring of elevated ICP is crucial. Clinically, intraventricular catheter and subdural screw are usually performed for ICP monitoring. However, these methods have unavoidable flaws such as the risks of brain hernia and low measurement accuracy. In recent years, as another current clinical available measurement method, minimally *invasive* surgery using various transducer systems stands a high importance in medical treatment field for cardiovascular, urodynamic, and hemodynamic surgery. Miniature pressure transducers based on piezoelectricity or optical fiber can be used *in vivo* medical treatment. Fiber optical sensors, compared to their counterparts, have the advantages of being immune to electromagnetic interference, having high sensitivity, and being lightweight[1,2].

To successfully measure ICP, the fiber optic sensor should have the following attributes: 1) biocompatibility; 2) miniature size; 3) adequate sensitivity, resolution, and dynamic range; 4) detection system to pick up subtle change of ICP. Thermal dependence is another non-negligible influential factor in the ICP measurement, especially for high precise measurement. In recent years, a variety of diaphragm-based Fabry–Perot (F-P) pressure sensors have been developed that can meet the high-sensitivity and resolution requirements of the ICP measurement[3–7]. In terms of the used diaphragm, the reported miniature F-P pressure sensor with adequate sensitivity can be classified as follows: graphene-based[3], metal-based[4], silica-based[5], and polymer-based[6,7]. For most of these sensors, the application prospect for the ICP measurement is limited either by its narrow-line pressure response range[3], susceptibility to oxidation[4], corrosion, high-temperature cross-sensitivity[6,7], or by its restriction in long-term liquid environment[6,7]. Among these sensors, all-silica F-P pressure sensors with a diameter of 125–250 μm have gained attention. Owing to the small size, these all-silica sensors are difficult to fabricate and handle. Consequently, various fabrication techniques for F-P pressure sensors have been shown recently. However, there are still some unavoidable limitations. Firstly, the length of the F-P cavity is hard to adjust during the fabrication[8–11]. Secondly, the fusion bond among the diaphragm, the lead-in optical fiber, and the outer sleeve are mostly implemented by a CO_2 laser bonding technique[12] or a propane torch[13]. These thermal bonding techniques are either costly or hard to handle. Besides that, the diaphragm of many miniature all-silica F-P sensors is made from a fiber whose diameter equals to the outer diameter of the outer sleeve[14]. In that case, the reflectivity of the diaphragm would contradict the firmness of fusion splices. Thirdly, because of small sensor dimensions and a high SiO_2 modulus of elasticity, outer sleeves with stepped inner diameters are customized to achieve practical sensitivity, which results in an increase of the complexity and cost of the fabrication[15].

In this letter, we present a miniature F-P pressure sensor with 220 μm outer diameter fabricated by simple techniques involving only cleaving, fusion splicing, and wet chemical etching to solve the earlier-mentioned problems. The length of the F-P cavity is easy to adjust by the manual operation of the fiber fusion splicer's motor. And the fusion bond among the diaphragm, the lead-in optical fiber, and the outer sleeve is completed by manual discharge of the fiber fusion splicer's electrodes. Our design could result in a better flatness of the diaphragm, which alleviates the contradiction between

the reflectivity of the diaphragm and the firmness of fusion splices and is conducive to reducing the thermal sensitivity compared with the method that bonding a fiber to the end face of a tube[16]. In addition, the online monitoring of the F-P cavity is actualized that will help us to find problems timely during the fabrication. Using commercially available silica glass tubes and fibers, the proposed all-silica sensor is extraordinarily low cost, is disposable, has low temperature sensitivity, is simple for fabrication, and is biocompatible and reliable, which gives rise to a great potential to be used in many fronts, especially for biomedical applications.

The cross-sectional view of the sensor element is shown in Fig. 1. It consists of a multi-mode (MM) optical fiber, a thin diaphragm, and a silica glass tube. The thin diaphragm is formed by inserting a fiber into a tube and splicing them together instead of bonding a fiber to the end face of the tube. Such a design would give rise to a better flatness of the diaphragm and a reduced thermal sensitivity. Thus, the polished end face of the fiber and the thin diaphragm form the F-P structure. The diameter of the cavity is determined by inner diameter of the silica glass tube, and the depth of the cavity is determined by the length of the air gap.

The fabrication method presented in this letter is shown in Fig. 2. Firstly, as shown in Fig. 2(a), a well-cleaved MM optical fiber (105/125 μm) or a coreless silica fiber serving as diaphragm is spliced to a silica glass tube (Sino Sumtech), having inner/outer diameter 128(+5)/220(±10) μm. Both fiber and tube are fixed into the V-type grooves of the fiber fusion splicer (FSM-60S; Fujikura). By manual operation of the splicer's motor, the optical fiber can be easily inserted into the silica glass tube, with approximately 20–40 μm overlap between the optical fiber and the silica glass tube. Then by the multiple manual discharging with a relatively low discharge capacity along the overlap, the optical fiber and the silica glass tube are well fusion bonded together. And multiple fusion splices along the overlap are formed, as shown in Fig. 2(e), where bonding point determines the reflectivity of the diaphragm and the firmness of the joint is mainly determined by other bonding points. Compared with the method that bonding a fiber to the end face of a tube[16], such design could result in a better flatness of the diaphragm and is conducive to reducing temperature sensitivity. Secondly, as shown in Fig. 2(b), a well-cleaved lead-in MM optical fiber (62.5/125 μm) is spliced to the earlier-mentioned silica glass tube. This second splice seals the F-P cavity. To monitor the length of F-P cavity in real time, we connected the lead-in MM optical fiber to the demodulation system. The accuracy of the adjustment system in the fusion splicer is 0.1 μm. So the length of the F-P cavity can be precisely controlled. Figure 2(f) shows that the quality of the F-P cavity can be monitored from the screen of the fusion splicer. Thus, if there are pollutants in the cavity or the flatness of the diaphragm is poor, these problems can be observed timely. This double-splicing operation forms the structure of the F-P cavity, where the two fibers enclose an air gap. Thirdly, as shown in Fig. 2(c), Thirdly, as shown in Fig. 2(c), the optical fiber is cleaved to serve as a diaphragm to retain a thin layer. serving as the diaphragm to retain a thin layer. Because of different diameters of the fiber and the silica glass tube, the cleaving point is so easy to find that cleaving can be accomplished without the aid of microscope, and the needed pulling force to perform cleaving is relatively small, as shown in Fig. 2(g). Finally, as shown in Fig. 2(d), the thickness of the diaphragm is reduced by wet chemical etching using hydrofluoric acid (HF). The

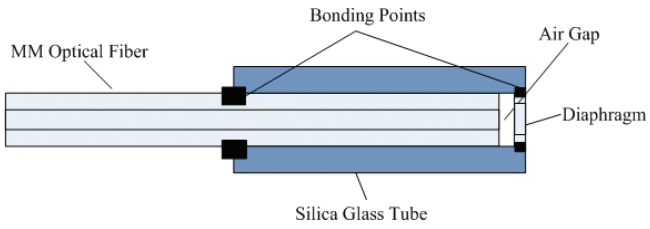

Fig. 1. Schematic structure diagram of the miniature F-P pressure sensor for biomedical applications.

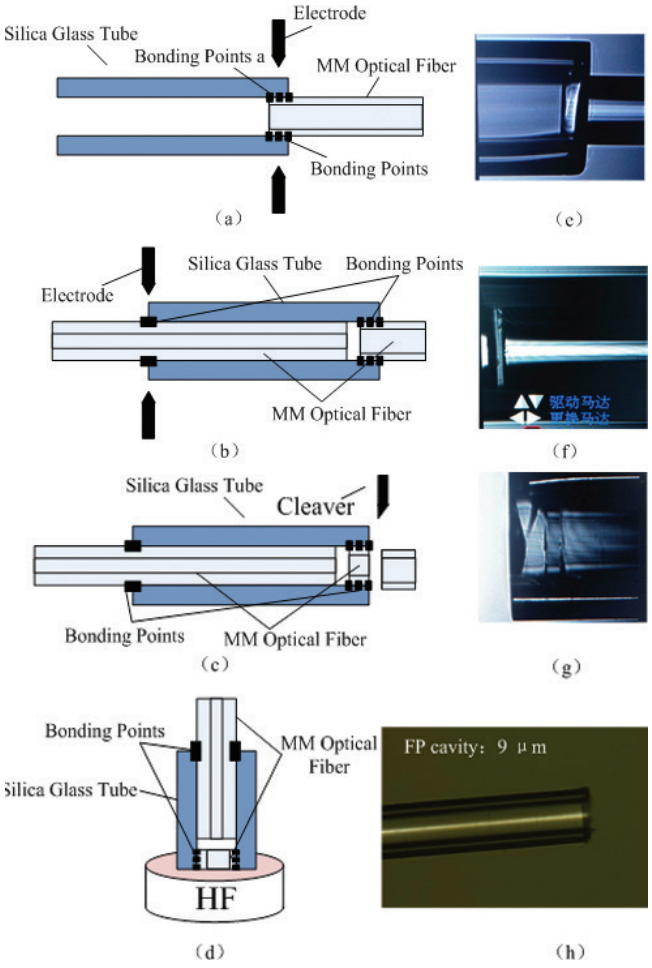

Fig. 2. The procedure of sensor fabrication. (a, e) Splice optical fiber serving as diaphragm and silica glass tube together. (b, f) Insert the MM optical fiber into the silica glass tube to adjust the F-P cavity and splice them together. (c, g) Cleave the optical fiber serving as diaphragm to retain a thin layer. (d) Minimize the thickness of the diaphragm by wet chemical etching using HF. (h) Micrograph of the completed sensor tip.

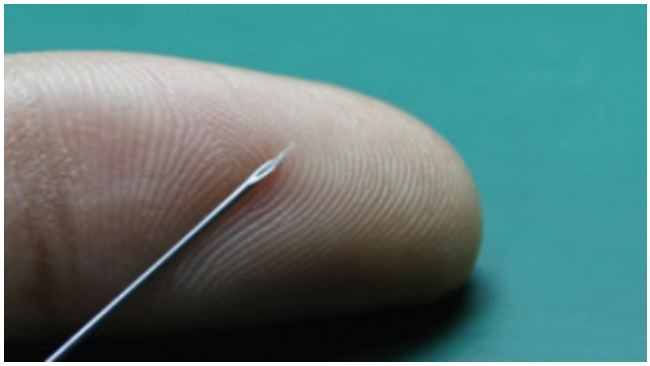

Fig. 3. Photograph of the pre-packaged F-P pressure sensor for the ICP measurement.

sensor tip can be polished before the chemical etching. To control the chemical etching process easily without destroying the thin membrane, we used buffered oxide etchant, instead of 40% HF, to minimize the thickness of the diaphragm, which is prepared by HF and ammonium fluoride (NH_4F) at different levels (0.2 μm/min etching rate at room temperature). Figure 2(h) is the micrograph of the completed sensor tip. From the aforementioned fabrication of the F-P sensor, an all-silica, epoxy-free, biocompatible and disposable F-P pressure is fabricated, which also solves the difficult art problems in diaphragm's connection and adjustment of the F-P cavity. To increase the mechanical strength of the F-P pressure sensor during the invasive measurement, the sensor can be packaged in a steel tube of 316 L, as shown in Fig. 3.

Figure 4 shows the schematic diagram of the experimental setup. The fiber optic sensor is placed in a sealed chamber in which the pressure is controlled by a pressure controller. The sealed chamber is filled with water to simulate the internal environment of the skull.

The demodulation system is based on white light interference principle. The key part (UMI-8; FISO) of the demodulation system is the Fizeau wedge used to reference F-P cavity. An incoherent white light source (600–1200 nm) is coupled into a circulator. Through the circulator, the light waves travel through the lead-in optical fiber until they reach its tip where the F-P interferometer pressure sensor is located. Light waves undergo multireflections in the F-P cavity of the sensor, whose length l is pressure P dependent. Then they travel back into the optical fiber. Through the

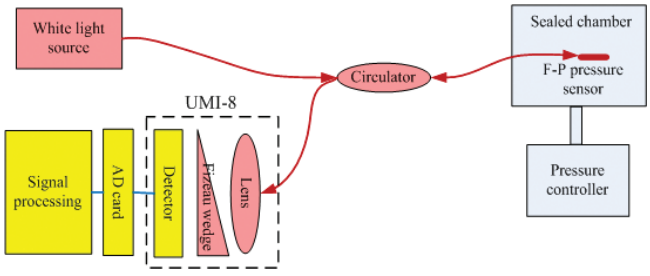

Fig. 4. Schematic diagram of the static experimental setup.

circulator, the reflected light is spread over a Fizeau wedge, which creates a linear variation of thickness, resulting in reconstruction of the interference pattern. The cross-correlated interference pattern, which is physically recorded using CCD, has a maximum intensity at the exact position the optical path difference equals the one created at the F-P pressure sensor. That is because the light source is white light, all wavelengths are present and thus destructive interferences occur except for the zero order where all wavelengths are actually constructive. Therefore, by finding the position of the maximum peak in the CCD, which is achieved with the AD card (NI-9215) with a resolution of 16 bit and through signal processing, the F-P cavity length l corresponding to the applied pressure P can be obtained from the following equation:

$$\Delta l = \frac{3\Delta P r^4 (1-\mu^2)}{16 E h^3}, \tag{1}$$

where Δl is the change of the F-P cavity's length and ΔP is the change of the external pressure applied

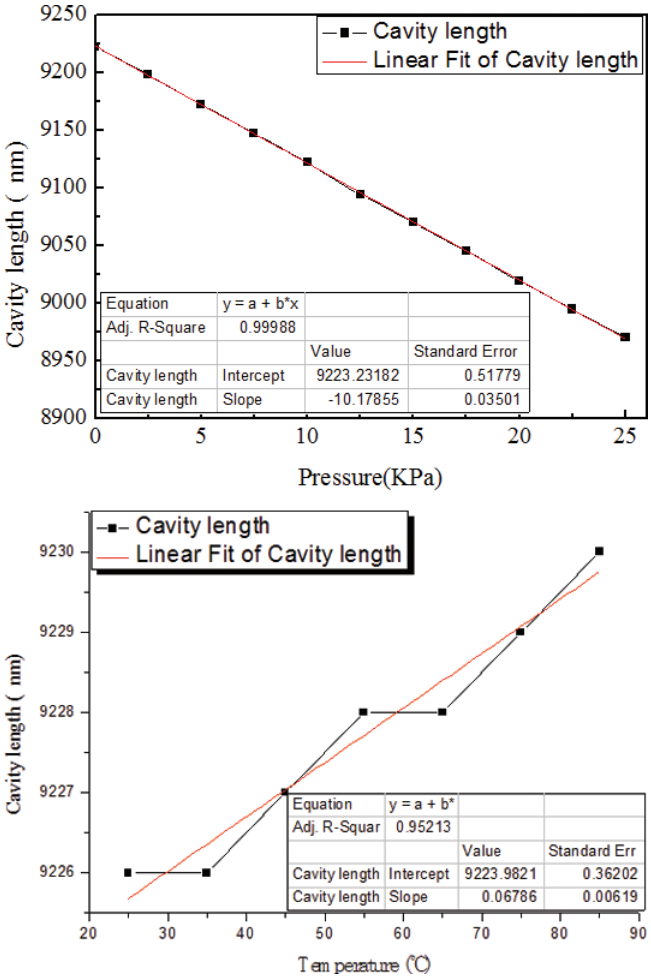

Fig. 5. Relation between pressure and cavity length of the sensor (upper). Relation between temperature and the cavity length of the sensor at constant pressure (lower).

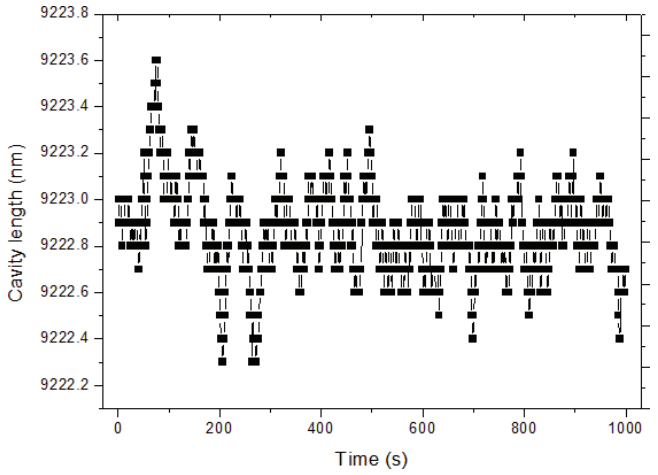

Fig. 6. Cavity length at constant temperature and pressure (sampling interval = 1 s).

to the diaphragm. In this case, for this all-silica sensor, the radius of the diaphragm r is 0.64 mm, the diaphragm's Poisson's ratio μ is 0.17, Young's modulus E is 73.73 GPa, and the thickness of the diaphragm h is reduced to be approximately 1.5 μm. Then the pressure sensitivity ($\Delta l/\Delta P$) of the proposed F-P sensor is calculated to be 12.28 nm/kPa. Temperature test is implemented by replacing the sealed chamber with thermostat.

Figure 5 (upper graph) shows the pressure experimental result, where the cavity of the sensor is plotted as a function of pressure. The fitting line is $l = 9223 - 10.18\,P$, the linearity is 99%, and the sensitivity is 10.18 nm/kPa with a resolution of 0.1 kPa, which can meet the requirements of the ICP measurement. Though body temperature variation is small, thermal dependence is still an important influential factor in the ICP measurement, especially for extremely precise measurement. Therefore, we take a temperature test on the 25–85 °C interval. Figure 5 (lower graph) shows the relation between temperature and the cavity length of the sensor at constant pressure. The experimental result shows that the thermal sensitivity of the proposed sensor is 0.068 nm/°C, resulting in a quite low ICP measurement error of 6.7 Pa/°C, which is tolerable in relation to the small body temperature variation during the ICP monitoring. Figure 6 shows data collection of the cavity length at constant pressure and temperature. Sampling interval is set to 1 s and 1000 data are acquired. The standard deviation of the cavity length is calculated to be 0.19 nm. Twice of standard deviation of the cavity length is regarded as the noise of the proposed sensor, the noise of the sensor can be as low as 37 Pa (corresponding to cavity length of 0.38 nm).

In conclusion, we present the design, fabrication techniques, and tests of a miniature, biomedical, low-cost F-P pressure sensor, which can be used for ICP monitoring or other medical applications. Sensor fabrication, which is completed only by a commercial fusion splicer and a fiber cleaver, is analyzed in detail, and it solves many difficult art problems involved in fabrication of compact F-P pressure sensor, including the adjustment of the F-P cavity, the bond problems among each sensor element. Compared with the method that bonding a fiber to the end face of a tube, our design could result in a better flatness of the diaphragm and is conducive to reducing temperature sensitivity. During the fabrication of the F-P cavity, the demodulation system connected to the lead-in fiber can help to monitor the optical characteristics of the cavity and the fusion splicer can help to monitor the geometrical characteristics of the cavity. The sensor exhibits a linear response to the applied pressure over the range of 0–25 kPa, with a sensitivity of 10.18 nm/kPa and a resolution of 0.1 kPa. The temperature test shows that the thermal sensitivity of the proposed sensor is 0.068 nm/°C on the 25–85 °C interval, corresponding to a quite low ICP measurement error of 6.7 Pa/°C, which is tolerable in relation to the small body temperature variation during the ICP monitoring. The proposed all-silica sensor meets the requirements of the ICP measurement and has a great potential to be used in many fronts, especially for biomedical applications. The next work is to take animal tests, make further improvement of the sensor resolution, and eliminate the effect of the atmosphere on the F-P pressure sensor for long-term measurement (over 24 h measurement).

This work was supported by Beijing Nova Program under Grant No. Z121101002512111.

References

1. D. D. John and P. W. S. Mark, J. Clin. Monit. **8**, 1 (1992).
2. X. Wang, N. Li, Q. Tan, and G. Jin, Chin. Opt. Lett. **6**, 925 (2008).
3. J. Ma, W. Jin, H. L. Ho., and J. Y. Dai, Opt. Lett. **37**, 2493 (2012).
4. F. Xu, D. Ren, X. Shi, C. Li, W. Lu, L. Lu, L. Lu, and B. Yu, Opt. Lett. **37**, 133 (2012).
5. N. Wu, Y. Tian, X. Zou, Y. Zhai, K. Barringhaus, and X. Wang, Sens. Actuators B Chem. **181**, 172 (2013).
6. H. Bae and M. Yu, Opt. Express **20**, 13 (2012).
7. Q. Wang and Q. Yu, Chin. Opt. Lett. **8**, 266 (2010).
8. X. W. Wang, J. C. Xu, Y. Z. Zhu, K. L. Cooper, and A. Wang, Opt. Lett. **31**, 7 (2006).
9. E. Cibula and D. Donlagic, Appl. Opt. **44**, 14 (2005).
10. D. Donlagic and E. Cibula, Opt. Lett. **30**, 16 (2005).
11. T. Cai, X. Tong, G. Chen, D. Wang, and Y. J. Rao, Proc. SPIE **8924**, 89242R (2013).
12. M. C. Li and Q. Y. Wang, in *Proceedings of Electronics, Communications and Control (ICECC)* 328 (2011).
13. W. H. Wang, N. Wu, Y. Tian, C. Niezrecki, and X. W. Wang, Opt. Express **18**, 9 (2010).
14. J. C. Xu, X. W. Wang, K. L. Cooper, and A. B. Wang, Opt. Lett. **30**, 24 (2005).
15. S. Poeggel, D. Tosi, G. Leen, and E. Lewis, Proc. SPIE **8797**, 87970B (2013).
16. K. Bremer, E. Lewis, and G. Leen, B. Moss, S. Lochmann, and I. A. R. Mueller, IEEE Sensors J. **12**, 1 (2012).